DESIGN AND EVALUATION OF AN ACTIVE VIBRATION ABSORBER

L. S. Hatcher, Jr.* and D. M. Egle

School of Aerospace and Mechanical Engineering, University of Oklahoma, Norman, Oklahoma

The conventional spring-mass vibration absorber can be used effectively for only a narrow band of exciting frequencies around its tuned frequency. The "active vibration absorber", by its ability to change its tuned frequency, is useful over a wider range of exciting frequencies. Previous work has been concerned with the formulation of possible control systems and with the experimental investigation of specific configurations for the active vibration absorber. This paper presents a design procedure, valid for any configuration, that indicates the proper absorber components for a particular application. The paper also reports on the investigation of a simple active vibration absorber.

Control of vibration is an important consideration in design work. Large displacements produced when a structure is excited at or near its natural frequency have been responsible for structural failures, and fatigue caused by vibration has resulted in other failures. But apart from complete structural collapse, uncontrolled vibration can result in high noise levels which can be very undesirable.

One method of controlling vibration is to use a vibration absorber. The basic theory behind the simple absorber is presented in most vibrations textbooks. Figure

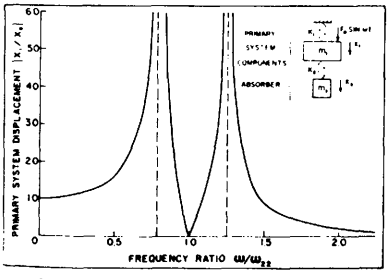

FIGURE 1. Typical behavior of a simple spring-mass absorber.

1 depicts a primary system which is forced to vibrate under the harmonic excitation $F = F_0 \sin \omega t$. By attaching a spring-mass system tuned to the frequency of the exciting force such that $\omega^2 = k_2/m_2$, the amplitude of the primary system can be greatly reduced, and the added spring-mass system acts as a vibration absorber. A typical plot of the response of the primary system, with the absorber attached, to a varying excitation frequency is shown in Figure 1. There are now two resonant frequencies of the system. This graph illustrates why a fixed spring-mass absorber is impractical. Although it absorbs the vibration at its tuned frequency, it does not function properly if the exciting frequency varies, even a small amount, from this set point. Because of this limitation, recent investigations have centered on an active vibration absorber that changes its natural frequency in order to keep the primary system response at a low level over a wide range of exciting frequencies.

There are a number of methods, both electrical and mechanical, to vary the natural frequency of an absorber (1-5). However, because of the complex and expensive control systems and/or excessive power requirements, these absorbers are not practical for all applications. Previous work has been concerned mainly with excitation frequencies in a range corresponding to the absorber natural frequency range. Often, the excitation frequency range may be greater than any practical absorber natural frequency range. Unless this fact is considered in absorber design, there will be two resonances of the primary system when the excitation frequency is outside of the absorber frequency range.

*Now Project Engineer, Celanese Chemical Company, Bay City, Texas.

Purposes of this paper are: (a) to present a design procedure for an active absorber that functions properly for an extended excitation frequency range (a range greater than the absorber natural frequency range); (b) to apply this procedure to the construction of a simple absorber system; and (c) to evaluate the effectiveness of the absorber for several types of exciting frequency variation.

DEVELOPMENT OF THE ABSORBER DESIGN

The basic configuration of the absorber used is shown in Figure 2. A cantilever

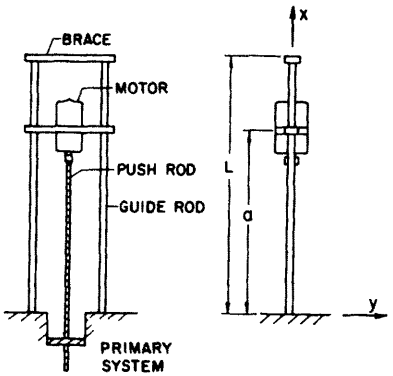

FIGURE 2. The absorber components.

with a movable mass was selected for the absorber. This arrangement is desirable because of its simplicity, and it also offers size and weight advantages over most other absorber types. The electric motor serves as the source of mechanical power for tuning the absorber system; it also serves as the movable mass. Several alterations may make the system more suitable for a particular application, e.g., use of a hollow-shaft motor, but the design procedure is valid for any configuration.

With the motor in any fixed position, the above system behaves essentially like the simple spring-mass absorber in Figure 1. The equations of motion corresponding to that system are

$$m_1\ddot{x}_1 = k_2(x_2-x_1) - k_1x_1 + F_0\sin \omega t$$
$$m_2\ddot{x}_2 = -k_2(x_2-x_1) \qquad \text{Eq. 1}$$

where

m_1 is the effective mass of the primary system,
m_2 is the effective mass of the absorber,
k_1 is the spring stiffness of the primary system, and
k_2 is the effective spring stiffness of the absorber.

By inserting the assumed solution to the forced vibration problem of $x_1 = X_1 \sin \omega t$ and $x_2 = X_2 \sin \omega t$, the equations of motion can be manipulated into the following expression for the amplitude of the primary system:

$$\frac{x_1}{x_0} = \frac{\left[1 - (\omega/\omega_{22})^2\right]}{\left[1 + k_2/k_1 - (\omega/\omega_{11})^2\right]\left[1 - (\omega/\omega_{22})^2\right] - k_2/k_1}$$

where $\omega_{22}^2 = k_2/m_2$,
$\omega_{11}^2 = k_1/m_1$, and
$x_0 = F_0/k_1$ Eq. 2

Equation 2 is the basis for the selection of the absorber components. First, however, the relationships for k_2, m_2, and m_1 must be developed in terms of the physical and geometrical properties of the particular absorber configuration being considered.

Rayleigh's method can be used to obtain these effective quantities for the natural frequencies of the primary system and the absorber at any motor position. An exact solution is impractical because of the complexity of the problem. The expressions for k_2, m_2, and m_1 are obtained for this absorber configuration in the Appendix.

It is now possible to examine the variation of the amplitude magnification factor X_1/X_0 with the exciting frequency for any set of absorber data and any position of the absorber mass. It is informative to inspect this variation with the absorber at its lowest and highest natural frequency positions. Figure 3 shows typical curves at these ab-

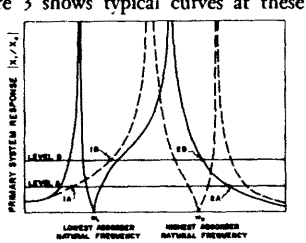

FIGURE 3. Primary system response curves with absorber at extremes.

sorber positions. (The curves are considerably distorted from the curve shown in Figure 1. This is because ω_{22}/ω_{11}.) These curves indicate that the absorber is capable of keeping $|X_1/X_0|$ below a certain level for any ω. For instance, the absorber is capable of keeping $|X_1/X_0|$ below Level B if at exciting frequencies below ω_L the absorber is tuned to its highest natural frequency, and if at exciting frequencies above ω_H it is tuned to its lowest natural frequency. For exciting frequencies in the absorber natural frequency range, the absorber can tune itself so that $\omega_{22} = \omega$, and in accordance with Equation 2, $|X_1/X_0|$ will be minimized. This absorber is not capable of keeping the magnification factor below Level A. At exciting frequencies between points 1a and ω_L the absorber is unable to find a position that will reduce $|X_1/X_0|$ sufficiently.

It can be seen that a condition for the absorber to function properly, *i.e.*, to keep $|X_1/X_0|$ below a certain specified level $|X_1/X_0|_{max}$ for an extended exciting frequency range, is that corresponding "cut-off" frequency points must be within the natural frequency range of the absorber. Points 1b and 2b, the cut-off points for Level B, lie between points ω_L and ω_H while points 1a and 2a do not.

A particular absorber is best utilized when the two cut-off points coincide with the low and high natural frequency points. Given a set of primary and absorber system data, it is possible to find this point of maximum utilization by altering the absorber configuration and the value of $|X_1/X_0|_{max}$. A computer program was devised which utilizes Equation 2 and the relationships for effective masses and stiffnesses to iterate to a design point near that of maximum utilization. The program yields the final absorber length and mass and final value of $|X_1/X_0|_{max}$.

Two parameters of importance in applying this device are the ratio of the absorber system mass to the primary system mass, and the value of $|X_1/X_0|_{max}$. Figures 4 and 5 indicate variations of these parameters for the primary and absorber systems used in this study. Each point in Figures 4 and 5

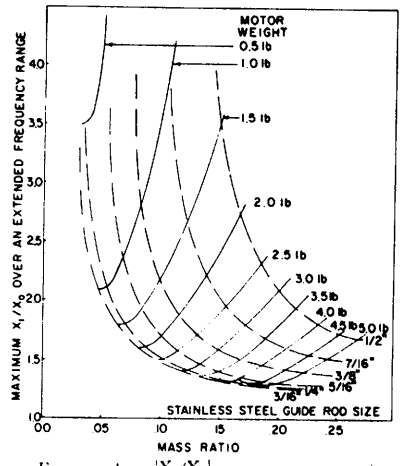

FIGURE 4. $|X_1/X_0|_{max}$ vs. mass ratio for various absorber data (stainless steel rods)

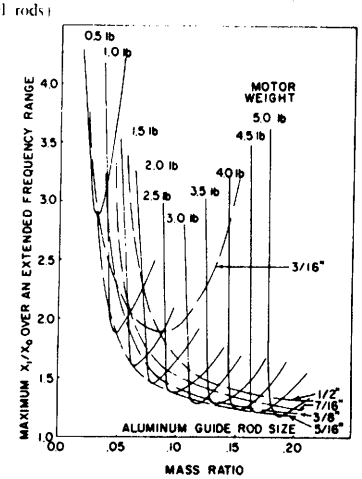

FIGURE 5. $|X_1/X_0|_{max}$ vs. mass ratio for various absorber data (aluminium rods)

corresponds to the best utilization of a particular absorber on the primary system. The original mass and spring constant of the primary system are the same for each point. Also, the sizes of the brace and the push rod, with the exception of its length, are

held constant. The remainder of the data varies as indicated in the figures.

Curves in Figure 5, where the guide rods are aluminum, indicate that a fixed weight motor is best suited to a particular size rod. This effect is less pronounced for the stainless steel guide rods in Figure 4.

Curves in these figures are independent of the magnitude of the exciting force. Hence, for a certain excitation, some of the absorber data points may be incompatible; *i.e.*, the guide rods may be unable to withstand the necessary force because they are improperly sized. This fact must be considered in the absorber selection.

Figures similar to 4 and 5 can be used effectively to determine an optimum absorber design. By checking the absorber compatibility, it is possible to obtain that absorber with the least value of $|X_1/X_0|_{max}$ for a specified mass ratio. In this case, for example, if the specified mass ratio is 0.08, Figure 5 yields the following possible values of the absorber components: a 2-pound motor on 3/16-inch rods; a 1.75-pound motor on 1/4-inch rods; a 1.4-pound motor on 3/8-inch rods; etc. Figure 6 yields other possible values. By examining the data sets in relation to their ability to withstand the necessary force, the best absorber can be selected. Conversely, the absorber with the least mass ratio can be obtained for a specified $|X_1/X_0|_{max}$.

One set of data in Figure 5 indicates that for this absorber and primary system, it is possible to obtain a value of $|X_1/X_0|_{max} = 3.8$ for a mass ratio of 0.023. For the primary system alone, $|X_1/X_0|$ can reach a value of slightly over 100 so that the reduction of the amplitude magnification factor is approximately 96% even for such a small mass ratio.

DESCRIPTION OF THE CONTROL SYSTEM

If the absorber is to function for any exciting frequency, it must match its natural frequency to the excitation frequency when ω is within the absorber range. It must tune its natural frequency to the upper limit when ω is just below the range, and tune its natural frequency to the lower limit when ω is just above the range. These requirements restrict the type of control systems that can be used. Recent work by Bonesho and Bollinger (3) on a self-adjusting absorber used a control system which kept the phase angle between the absorber and the main mass at 90 degrees. This system is operable only for exciting frequencies within the absorber range.

The control system adopted was previously used by Dunham and Egle (5). This system senses the amplitude of the primary mass and activates the absorber motor when this amplitude exceeds the design level. The motor then moves through the absorber frequency range until it finds the position where the primary system amplitude is sufficiently reduced.

This control system has one apparent weakness: it is not sensitive to the direction that the absorber motor should move for the amplitude reduction. For certain changes in exciting frequency, the motor may have to travel to the end of the guide rods and back before it is properly positioned. This may cause temporary instability in the primary system amplitude.

This control system has two desirable features. First, the system responds directly to the amplitude of the primary system. Second, the control system is extremely simple and inexpensive. The phase angle control system previously mentioned requires sophisticated equipment. In its simplest form, this system, shown in Figure 6(A), requires only a power supply and

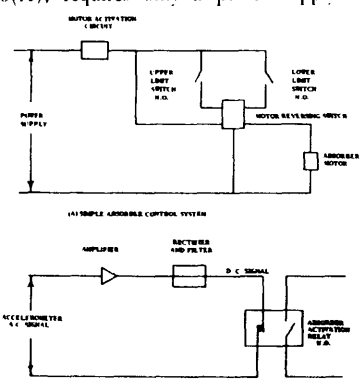

FIGURE 6. Absorber control system.

appropriate switches. A piezoelectric accelerometer mounted on the primary mass was used to activate the absorber as shown in Figure 6(B). A mechanical vibration switch in place of the activation circuit would simplify the control system.

EXPERIMENTAL EVALUATION

The primary and absorber systems used in this experimental investigation can be seen in the photograph in Figure 7. The

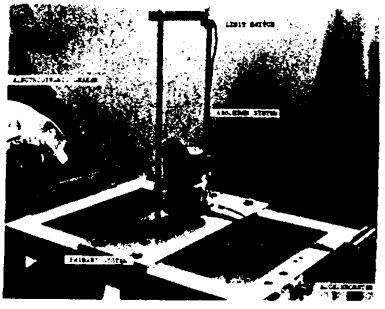

FIGURE 7. Prototype primary and absorber systems.

primary system consists of a framework mounted on four flat bars and coupled to an electrodynamic shaker. The shaker provides the excitation through the coupling spring, and the legs provide the restoring force. The mass m_{pr} of the primary system consists of the mass of the framework plus the proper percentages of the spring masses. The spring constant of the system, k_1, is equal to the spring constant of the legs plus that of the coupling spring. With these definitions this system approaches the primary system model of Figure 1 used in the design.

The absorber was constructed in accordance with the configuration of Figure 2. The movable mass is an instantly reversible d.c. motor with a weight of 2.26 pounds. The guide rods are 1/4-inch stainless steel. The application of the design procedure described previously indicated that for these components the absorber would function best for a value of $|X_1/X_0|_{max} = 1.55$ and a mass ratio of 0.096. These values can be checked in Figure 5.

The curves in Figure 8 are presented as a verification of the absorber design. Curve

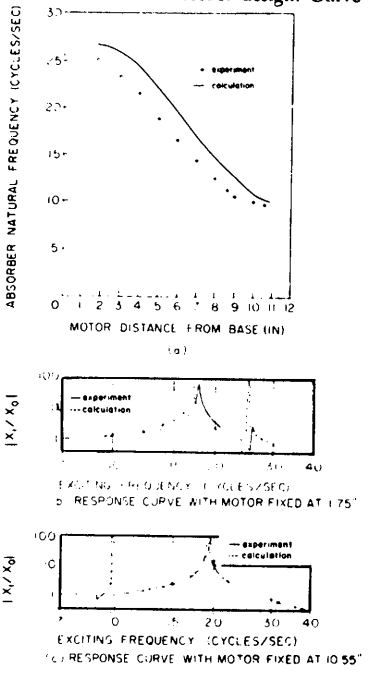

FIGURE 8. Experimental verification of absorber design.

(a) compares the calculated absorber natural frequencies for various motor positions with the experimental values which were determined by varying the exciting frequency until the primary system amplitude was minimized and by using the fact that $\omega_{22} = \omega$ at this point. The agreement is not close at all motor positions. However, at the motor limits (at 1.75 inches and at 10.55 inches) the error is well below 10%. The natural frequency equation was formulated in a manner yielding close agreement at the motor limits because these are the absorber design points.

Curves (b) and (c) compare the experimental and the calculated plots of $|X_1/X_0|$

versus ω at the design points. For complete validity, the absorber natural frequency range used in the design must be within the actual range. Using Rayleigh's method, the actual absorber natural frequencies will always be less than those calculated. Therefore, the calculated value for the low frequency is acceptable in the design, but the high calculated frequency must be reduced to a level below the actual value. This was accomplished by decreasing the calculated frequency by 10%. This reduction accounts for the fact that in the calculated plot of curve (b) ω does not coincide with the calculated value of ω_{22} at the point of minimum $|X_1/X_0|$. An examination of the actual experimental curves indicates that the critical design points are within the limits needed for proper absorber operation.

The results of the first test conducted to determine the absorber effectiveness are shown in Figure 9. The top curve in each

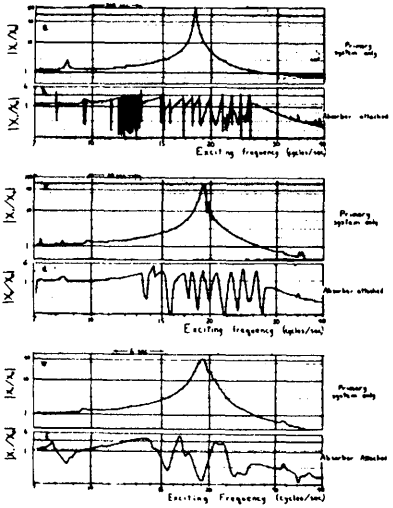

FIGURE 9. Response of the primary system, with and without the active absorber, to increasing excitation frequencies.

set of plots gives the response ($|X_1/X_0|$) of the primary system alone to an increasing excitation frequency. The second curve gives the response under the same increasing frequency when the absorber was attached and operating.

Curves (a) and (b) correspond to the slowest rate of increasing frequency. The ratio $|X_1/X_0|$ reaches a value of near 100 for the primary system alone, while with the absorber attached the response remained below 5 for a 95% reduction. Although the absorber was rated for a $|X_1/X_0|_{max}$ of 1.55, the device could not be activated at this level because of the hysteresis of the activation relay [Figure 6(b)]. The motor had to be activated at a value of $|X_1/X_0|$ slightly greater than 2 so that it would deactivate when $|X_1/X_0|$ returned below 1.55. The low points in the curves after each motor activation are due in part to a momentary decrease in the level of excitation. This was caused by a lag in the control system of the electrodynamic shaker. Peaks in curves that exceed the turn-on value of the absorber generally occurred where the motor was required to make a large position or direction change.

Curves (c) and (d) reflect a more rapid rate of increase in exciting frequency. The resonant peak of the primary system in this case dropped to a value of $|X_1/X_0| = 60$. With the absorber attached this response remained below 5 for a 91% reduction.

Curves (e) and (f) again show the absorber functioning properly. For this rate of frequency increase the amplitude reduction was approximately 88%.

Figure 10 shows the primary system re-

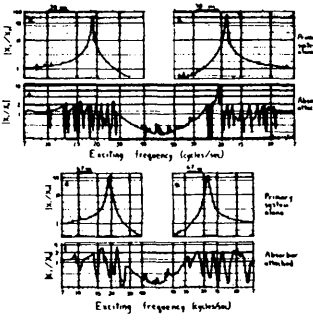

FIGURE 10. Response of the primary system with and without the active absorber, to increasing and then decreasing excitation frequencies.

sponse to an increasing and then decreasing exciting frequency. The two upper curves in each set were taken without the absorber attached, while the lower curve was taken with the absorber attached and operating.

Curves (a), (b), and (c) correspond to a relatively slow rate of frequency change. With the exception of one peak in the primary system amplitude, the absorber functioned as intended. This peak occurred again when the motor had to travel to the absorber limit, reverse itself, and return to the proper position. Even in this adverse situation, the reduction in $|X_1/X_0|$ was approximately 84%.

The exciting frequency varies more rapidly for curves (d), (e), and (f). It changed rapidly enough that the primary system did not fully respond to the second resonance peak with the absorber motor in its highest natural frequency position. This probably occurred because the resonant peak is relatively small as indicated in Figure 8(b). The result was that as the exciting frequency increased beyond the absorber range, the motor remained at the highest frequency position instead of returning to the low frequency end. Therefore, when the exciting frequency began to decrease the motor was in the proper position and was headed in the proper direction. This is why the instability peak of curve (c) is absent in curve (f). The corresponding reduction in $|X_1/X_0|$ was approximately 93%.

The results of another type of test which was used in evaluating this absorber system are given in Figure 11. The procedure used

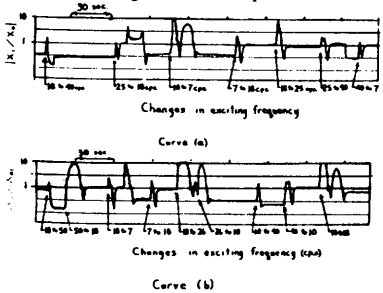

FIGURE 11. Response of the primary system, th the active absorber, to step changes in exciting quency.

in this test was to change the exciting frequency as rapidly as possible (nearly instantaneously) and record the associated response of the primary system as the absorber readjusted itself. When equilibrium was achieved another frequency change could be made. As can be seen from the curves, a majority of the frequency changes were focused around 18 cps, which is the approximate natural frequency of the primary system alone. Changes to and from this frequency caused the greatest instability; therefore, these changes are of particular interest.

Considering the range of frequencies involved, the absorber functioned very well for the arbitrary frequency changes; for the most part it kept $|X_1/X_0|$ below 10 and readjusted itself in an average time of less than 10 seconds. In some cases the absorber had to activate twice to get $|X_1/X_0|$ back to a completely stable position. This was due to the region of instability in the motor activation relay. Two peaks in curve (b) drove the recording pen to its upper limit and do not reflect the true values of the response.

It is interesting to note that although the absorber is designed to keep $|X_1/X_0|$ less than 1.55, the usual equilibrium point is considerably less than this value.

This absorber did not function well in all the tests. Two examples are shown in Figure 12. The set of curves (a), (b),

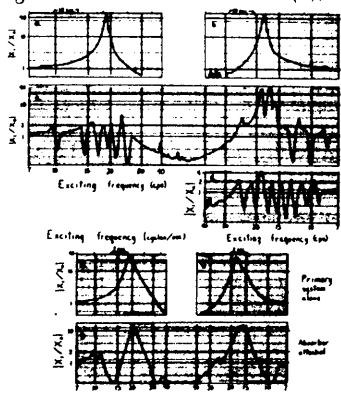

FIGURE 12. Absorber instabilities.

and (c) and the set of curves (e), (f), and (g) are the results of tests conducted in the same manner as before (Figure 10) but with different rates of exciting frequency change. The rate of frequency change for curves (a), (b), and (c) was between that of the two sets in Figure 10. In this case, as the exciting frequency increased beyond the absorber range, the motor adjusted back toward its lowest frequency position. When the exciting frequency began to decrease, the motor had to complete the cycle to its low frequency limit, return to its high frequency limit, and adjust back to the proper position. The result of this wasted motion was the instability shown in curve (c) where $|X_1/X_0|$ increased almost to the level of the maximum value of $|X_1/X_0|$ for the primary system alone.

One possible method to avoid the instability in curve (c) is to change the motor direction when the exciting frequency reverses its direction of change. Curve (d) illustrates this point. The initial motor positions for curve (d) and for the corresponding part of curve (c) were the same. However, the motor direction was reversed for curve (d). It can be seen that the instability was eliminated. If in an application the exciting frequency is controlled by some type of throttle, this means of aiding the system stability might be practical.

Curves (e), (f), and (g) were obtained for a very rapid rate of frequency change. In this case the absorber was able to reduce $|X_1/X_0|$ by only 50%.

As mentioned before, the control system used in this work has several desirable features and one major weakness. The weakness in the system is that it cannot send the motor in the right direction. If the motor has to travel a relatively large distance before it finds the tuned position, another factor becomes important, i.e., the speed of the absorber motor. The results of the tests presented in this section indicate that $|X_1/X_0|$ does increase when the absorber motor is forced to move a great distance. It is natural to assume that by increasing the motor speed these instability peaks can be narrowed but there is a limit to the allowable motor speed. The primary system must respond rapidly enough when the motor reaches its tuned position to deactivate the system. This response time appears to be the limiting factor because if it is too great the absorber will have passed its tuned position before the system can be deactivated.

CONCLUSION

If the frequency of the harmonic force on the primary system varies too rapidly or continuously, this absorber will not function. A more complex absorber or damper must be used. If the exciting frequency changes only occasionally and at a slow rate, this absorber will function well. If short-duration amplitude increases are acceptable, the absorber can be used effectively on systems subjected to an occasional step change in exciting frequency. The effectiveness of this absorber for excitations other than simple harmonic is unknown.

APPENDIX

Rayleigh's method requires the assumption of a deflection curve for the system. This is difficult since the curve depends on the position of the motor. When the motor is against the base, the deflection curve of the vibrating rods is similar to the static deflection curve of a cantilever subjected to a point load at the end. This assumption holds when the motor is at the free ends of the rods also. Therefore, the assumed deflection curve for the guide rods is

$$y = Dx^2(3L-x) \sin \omega t \quad \text{Eq. A-1}$$

where x and y are the coordinates defined in Figure 2. Equation A-1 is a good assumption for the deflection curve of the push rod except the amplitude should be something less than D. In general however, the error introduced by using the same amplitude should be slight. A better assumption can be made when more accuracy is required.

The potential energy U stored in the rods due to bending is

$$U = 2\int_0^L \frac{1}{2} FI_g (d^2y/dx^2)^2 \, dx + \int_0^a \frac{1}{2} FI_p (d^2y/dx^2)^2 dx$$

Eq. A-2

Using equation A-1 as the assumed deflection, the maximum potential energy reduces to the form

$$T_{max} = 12\,D^2\left[EI_g L^3 + \frac{1}{2}\,EI_p a(a^2 - 3La + 3L^2)\right] \quad \text{Eq. A-3}$$

The kinetic energy T of the system is

$$T = 2\left[\int_0^L \frac{1}{2} m_g \dot{y}^2 dx + \int_0^a \frac{1}{2} m_p \dot{y}^2\, dx + \frac{1}{2} M_m \left[\dot{y}^2\right]_{x=L} + \frac{1}{2} I_m \left[\dot{\phi}^2\right]_{x=a} + \frac{1}{2} I_b \left[\dot{\phi}^2\right]_{x=1}\right] \quad \text{Eq. A-4}$$

Again using Equation A-1 as the assumed deflection, the maximum kinetic energy reduces to the following form

$$T_{max} = \omega^2 D^2\left[\frac{33}{35} m_g L^7 + \frac{33}{70} m_p a^7 + \frac{1}{2} M_m a^6 (3L-a)^2 + 2M_b L^6 + \frac{9}{2} I_b L^4 + \frac{9}{2} I_m a^2 (2L-a)^2\right] \quad \text{Eq. A-5}$$

Equating $T_{max}=U_{max}$ and manipulating yields the following expression for the first mode natural frequency of the absorber system

$$\omega_{22}^2 = k_2/m_2 \quad \text{Eq. A-6}$$

$$k_2 = \frac{6EI_g}{L^3} + \frac{3EI_p}{L^6}(a^2 - 3La + 3L^2), \text{ and}$$

where , and Eq. A-7

$$m_2 = \frac{33}{70} m_g L + \frac{33}{140} m_p \frac{a^7}{L^6} + \frac{1}{4} M_m \frac{a^6}{L^6}(3L-a)^2 + M_b + \frac{9}{4} I_m \frac{a^2(2L-a)^2}{L^6} + \frac{9}{4L^2} I_b \quad \text{Eq. A-8}$$

It is interesting to note that when a=O, $k_2 = (6EI_g / L^3)$. This is twice the value of the accepted spring constant of a cantilever beam, as it should be.

The only remaining relationship needed is that for m_1. This can be calculated as follows

$$m_1 = m_p + m_a - m_2. \quad \text{Eq. A-9}$$

REFERENCES

1. A. K. Abu-Akeel, Trans. Amer. Soc. Mech. Engr. 89, Ser. B, (J. Engr. Indus.): 741-753 (1967).
2. J. A. Bonesho and J. G. Bollinger, Machine Design 40: 123-127 (1968).
   ----------, Theory and Design of a Self-Optimizing Damper, Proc. 7th Internat. Machine Tool Design and Research Conf., Birmingham, England, 1966, pp. 229-241.
   T. D. Dunham, Experimental Investigation of an Active Vibration Absorber, M.S. Thesis, University of Oklahoma, Norman, 1968.
   T. D. Dunham and D. M. Egle, Shock and Vibration Bulletin 38: 235-241 (1968).

NOTATION

- a —distance from base of guide rods to motor
- D —arbitrary amplitude in assumed deflection curve for absorber
- EI_g —flexural rigidity of the guide rods
- EI_p —flexural rigidity of the push rods
- F —excitation force on primary system
- F_0 —magnitude of harmonic force on primary system
- I_m —mass moment of inertia of the motor about an axis through its guides
- I_b —mass moment of inertia of the brace about an axis through its mounting brackets
- k_1 —spring stiffness of the primary system
- k_2 —effective spring stiffness of the absorber
- m_a —total mass of the absorber components
- m_g —mass/unit length of the guide rod
- m_p —mass/unit length of the push rod
- m_{pr} —original mass of the primary system before the absorber is attached
- m_1 —effective mass of the primary system with the absorber attached
- m_2 —effective mass of the absorber
- M_b —mass of the brace
- M_m —mass of the motor
- t —time coordinate (sec)
- T —kinetic energy of absorber
- T_{max} —maximum kinetic energy of absorber
- —potential energy of absorber
- U —maximum potential energy of absorber
- U_{max} —coordinate along the length of the guide rods [Figure 2]

x —static deflection, F_0/k_1

X_0 —displacement of primary effective mass from equilibrium [Figure 1(a)]

x_1 —amplitude of vibration of the primary effective mass

X_1 —displacement of the absorber effective mass from equilibrium [Figure 1(a)]

x_2 —primary system amplitude magnification factor

X_1/X_0 —deflection coordinate of absorber system, Figure 2

y —$\tan^{-1}(dy/dx)$

φ —frequency of the excitation force (radians/sec)

ω —point in Figure 3 corresponding to the highest absorber natural frequency

ω_H —point in Figure 3 corresponding to the lowest absorber natural frequency

ω_L —$\sqrt{k_1/m_1}$

ω_{11} —$\sqrt{k_2/m_2}$

ω_{22} —cut-off points corresponding to Level A in Figure 3

1a, 2a, 1b, 2b —cut-off points corresponding to Level B in Figure 3